Diatom Research 31: 231-242

Morphometric allometry of representatives of three naviculoid genera throughout their life cycle

KATERINA WOODARD , JANA KULICHOVÁ, TEREZA POLÁCKOVÁ & JIRÍ NEUSTUPA

Department of Botany, Faculty of Science, Charles University in Prague, Benátská 2, Praha 2 12801, Czech Republic

The frustule architecture of diatoms and the nature of the vegetative cell division phase of their life cycle constrain cell size and shape. For decades, diatomists have observed that size diminution is accompanied by valve shape changes. However, allometric shape changes have rarely been assessed using quantitative statistical tools. In the present study, we employed geometric morphometrics to examine the shape dynamics of raphid diatom frustules. An investigation was carried out to explore whether shape characteristics, such as circularity or asymmetry, and variation of valve outline, increase with decreasing cell size. Four monoclonal strains (*Luticola dismutica* strain 1, *L. dismutica* strain 2, *Navicula cryptocephala*, and *Sellaphora pupula*) were cultivated under stable conditions for two years in order to capture the complete range of cell sizes from initial to sexually competent cells. Shape changes and the pattern of shape change relative to size were quantified using geometric morphometrics. A quantitative shape analysis revealed similar allometric trends among the different strains and genera. With decreasing cell size, circularity of the valve outlines increased, that is, the complexity of the valves decreased. However, shape variation of valves within the populations increased with decreasing cell size. The levels of asymmetry did not change consistently throughout the size diminution phase. In two out of four strains, horizontal (dorsiventral) asymmetry was significantly lower than vertical (heteropolar) and transversal (sigmoid) asymmetries. The increasing morphological variation in clonal strains was likely caused by an accumulation of structural deviations during morphogenesis. In this respect, this is a specific example of the structural inheritance of morphological characteristics, which is naturally related to the peculiar vegetative life cycle of the diatoms.

Keywords: *allometry, geometric morphometrics, life cycle, raphid diatoms, plasticity*

Introduction

Diatoms are ubiquitous unicellular algae with a unique morphology. The siliceous cell wall (frustule) of diatoms consists of two complementary valves. In simple terms, the epivalve fits over the hypovalve in the same way as a lid fits over a bottom of a Petri dish. When the cell divides, new valves and bands develop inside the orig-inal valves. Therefore, the old hypovalve becomes the epivalve of the new frustule. It is apparent that, over time, this process leads to mean cell size diminution in a clonal population. MacDonald (1869) and Pfitzer (1869) each independently described this peculiarity, and it is now known as the MacDonald–Pfitzer hypothesis (Koci-olek & Stoermer 2010). Even though there are mechanisms to avoid it (Lewis 1984, Edlund & Stoermer 1997), most diatom species appear to break out of the size diminu-tion via sexual reproduction. According to Geitler (1932), the condition necessary for initiating the sexual process is reaching a minimum cell size. This so-called *first cardi-nal point* of the diatom life cycle is defined as a size at which the cells can be induced to become gametangia. In pennate diatoms, this is typically when cell size is around 30–40% of the maximum size (Drebes 1977). The *second cardinal point* is reached after sexual reproduction occurs (Geitler 1932). At this point, cells restore themselves to the largest size they can achieve during their life cycle. Enlargement occurs through auxospore formation, a spe-cial zygote in which the initial epivalve and hypovalve develop. The new valves are formed below the surface of the auxospore. Therefore, initial cells have a rather differ-ent morphology to typical vegetative cells. Interestingly, cells that contain initial valves discontinue dividing after a few divisions and disappear from the population (Edlund & Stoermer 1997). The vegetative cell division phase of a population can take several years or even decades (Round et al. 1990). As the population mean approaches the mini-mum cell size, some cells miss the opportunity for sexual reproduction and continue to divide vegetatively, and, as a result, continue to diminish in size. These extremely small cells are often teratological and their pervalvar axis is sev-eral times greater than that in the normal vegetative cells (Geitler 1932). They are not viable under natural condi-tions but they can survive for a while in culture (Geitler 1932).

The unique characteristic of the diatom life cycle is that, unlike other organisms, their mean body (cell) size (in a clone) decreases over time. During this period, non-proportional shape change of the diatom frustule outline

has been described (Geitler 1932, Tropper 1975, Theriot & Ladewski 1986, Cox 1993, Schmid 1994, Edlund & Stoermer 1997, Mann & Chepurnov 2005, Veselá et al. 2009, English & Potapova 2012). As the number of cell divisions increases, cells of a number of species lose undulations and their outlines become more elliptical. In centric diatoms, the ratios of various elements change as the cell diameter changes (Theriot et al. 1988). These shifts can be con-nected to a loss of taxonomically important characteristics (Schmid 1994), and species determination may be difficult (Rhode et al. 2001, Pappas & Stoermer 2003, Fránková et al. 2009). Populations at different size diminution stages in the life cycle can also be misinterpreted as different species (Cox 1986, Rose & Cox 2014). The size diminution during the vegetative phase of the life cycle presumably affects the metabolism of the cells. Geitler (1932) proposed that the size influences protoplast organization. According to Schmid (1994), 'the ratio of the volume of the nucleus, cytoplasm, and vacuole also changes, leading to the physi-ological and subsequently the morphological heterogeneity of a clonal population' (Schmid 1994). Schmid (1994) also noted that 'during the vegetative cell division phase, the epivalves serve as a mold for the newly synthetized hypo-valves'. Therefore, some inaccuracies that arise during morphogenesis can be passed on to the next generation.

In past decades, numerous diatomists have focused on this phenomenon. Geitler's monograph (1932) contains comprehensive, qualitative observations of the diatom life cycle in both natural and laboratory conditions, and is a pioneering study in the field. More recently, researchers have used various quantitative methods for capturing the shape dynamics of diatom valves, such as the regression of the width and length (Tropper 1975), the Legendre shape analysis (Theriot & Ladewski 1986, Rhode et al. 2001, Pappas & Stoermer 2003, Mann et al. 2004), and the Fourier analysis (Mou & Stoermer 1992, Pappas et al. 2001). Landmark-based geometric morphometrics were found to be inadequate for diatoms at first, because they lack homologous points (Mou & Stoermer 1992). For studying landmark-poor outlines, Bookstein (1997) intro-duced a sliding semi-landmark method. After the usual translating, scaling, and rotating landmarks, the semi-landmarks are slid along the outline until they match the curve between two corresponding points as accurately as they can (Adams et al. 2004). The Procrustes superimpo-sition, based on semi-landmarks, has been established in a wide range of biological studies. With respect to diatoms, the semi-landmark method was used to explore morpho-logical variability within the *Achnanthidium minutissi-mum* species complex (Potapova & Hamilton 2007). The landmark-based shape analysis was employed to study the morphology and ontogenetic allometric trends of several taxa in the genus *Surirella* (English & Potapova 2012). Recently, it was also used to compare the ontogenetic allometric trajectories of valve outline and several other continuous variables with respect to the diagnoses of three species of *Pinnunavis*, a raphid genus allied to *Pinnularia* and *Navicula* (Edgar et al. 2015).

In the present study, landmark-based geometric morphometrics are used for exploring the patterns of shape variability and for the quantification of allometric and non-allometric shape changes of raphid diatoms cultivated under laboratory conditions. Our aim was to describe and quantify the general patterns of the shape dynamics con-nected to the diatom life cycle. In this sense, our study continues Geitler's (1932) approach, except that we used modern methods of quantitative shape analysis that were unavailable in his time. According to qualitative observa-tions (Round et al. 1990, Mann 1999), the valve outline becomes simpler with the increasing number of vegetative cell divisions, and so our aim was to quantify the relation-ship of valve complexity and valve size. Our hypothesis was that, throughout the asexual life cycle, valve com-plexity decreases as valve size decreases. We assumed that the morphological variation within populations and the asymmetry of valves would increase due to the grad-ual accumulation of developmental inaccuracies during valve morphogenesis. We measured the complexity, dis-parity, and asymmetry of the valves within clonal popula-tions in relation to valve size. Rather than species-specific patterns, we attempted to look for trends that are simi-lar across different genera of commonly occurring raphid diatoms, in order to identify the general laws involved in the morphological dynamics of the diatom valve.

Materials and methods

Cultivation and microscopy

Four monoclonal strains of raphid diatoms, obtained from Prof. A. Poulícková,ˇ Palacký University Olomouc, were used in this study. The strains examined were *Luti-cola dismutica* (Hustedt) D. G. Mann (strains LUTM 59 and LUTM 48, [Poulícková ˇ 2008]), *Navicula cryp-tocephala* Kützing, and *Sellaphora pupula* (Kützing) Mereschkowsky. All the strains were homothallic, so they undergo sexual reproduction within a monoclonal culture.

All four strains were cultivated from November 2009 to October 2011 to capture the entire size range of the cells throughout the life cycle. The strains were culti-vated in liquid WC medium (Andersen 2005), at 18°C in 7 cm diameter Petri dishes , illuminated at 40 µmol m^{-2} s^{-1} from 18 W cool fluorescent tubes (Phillips TLD 18W/33). The medium was replaced every week in order to avoid exhaustion of nutrients. Once every month, approximately 10% of the cells were transplanted to new Petri dishes in order to avoid overcrowding of cells. Every two months, samples were taken from the cultures and processed for the light microscopy analysis. The valves were cleaned in beakers by oxidation with 35% hydrogen peroxide and sev-eral crystals of potassium dichromate for 15 minutes, fol-lowed by several washings with distilled water (Poulícková ˇ 2008). The clean valves were then mounted in Naphrax,

Table 1. The size group delimitation, designation of size groups, number of specimens in size groups, and a size range of size groups in μm.

Strain	Size group % from the biggest cell length	Size group designation	Number of speci-mens	Size range (μm)
Luticola 1	100–90%	1	25	41.0–36.9
	90–80%	2	25	36.8–32.8
	80–70%	3	25	32.7–28.7
	70–60%	4	25	28.6–24.6
	60–50%	5	24	24.5–20.5
	50–40%	6	25	20.4–16.4
Luticola 2	100–90%	1	20	38.9–35.0
	90–80%	2	25	34.9–31.2
	80–70%	3	25	31.1–27.3
	70–60%	4	25	27.2–23.4
	60–50%	5	25	23.3–19.5
	50–40%	6	24	19.4–15.6
	40–30%	7	25	15.5–11.7
Navicula	100–90%	1	25	46.6–42.0
	90–80%	2	25	41.9–37.3
	80–70%	3	25	37.2–32.6
	70–60%	4	25	32.5–27.9
	60–50%	5	25	27.8–23.6
Sellaphora	100–90%	1	25	38.7–34.8
	90–80%	2	25	34.7–30.9
	80–70%	3	25	30.8–27.1
	70–60%	4	25	27.0–23.2
	60–50%	5	25	23.1–19.3

as described in Poulícková˘ & Mann (2006). The cultures were sampled until the complete range of valve sizes was captured and the auxosporulation and size restoration were observed.

Micrographs of 50 valves from each permanent slide (i.e. a sample corresponding to a certain life-cycle stage in a culture) were obtained using an Olympus BX-51 light microscope fitted with an Olympus Z5060 digital camera. The digital micrographs were compiled in Adobe Photo-shop CS3 ver. 10.0 and a number of valves were randomly chosen for statistical analyses. Size groups were used only for the analysis of partial disparity (i.e. morphological variability) in different stages of the life cycle and were determined based on the intervals of 10% of the maximal valve length (Table 1).

Statistical analysis

Geometric morphometric analyses were performed using the TPS-series software (Rohlf 2013). The shapes of the valves were registered in TpsDig, ver. 1.45. In total, 32 landmarks were positioned along the valve outline. Four landmarks were in fixed positions (nos 1–4: intersection of the valve outline with the apical and transapical axes) and the remaining 28 landmarks were allowed to slide along the outline between the fixed landmarks (5–11; 12–18; 19–25; and 26–32). The valves of all four strains were symmetrized along both the apical and the transapical axes. This was because left–right valve orientation could not be clearly determined from the micrographs, which focused primarily on the valve outline. Due to the symmetriza-tion, the asymmetric component of shape variation was eliminated from the data, and except for the decomposi-tion of the symmetric and asymmetric components of the shape variability, subsequent analyses were performed on symmetric configurations (Klingenberg et al. 2002).

The Procrustes superimposition was conducted in TpsRelw, ver. 1.46. Following that, the thin-plate spline analysis, based on tangent space projections (Bookstein 1997, Zelditch et al. 2004), was performed. Principal com-ponent analysis (also called the relative warp analysis) of partial warps and uniform components was conducted for each strain separately in TpsRelw, ver. 1.46. The first two relative warps were plotted against each other in order to illustrate the shape changes among cells in the individual strains. Deformation grids based on the thin-plate spline interpolation (Zelditch et al. 2004) represented the mar-gins of the realized morphospace on a particular warp in each strain. To capture the size-to-shape patterns of indi-vidual strains, we conducted multiple regressions of shape coordinates using a quarter of the symmetric coordinates (landmarks 1; 3; 5–11) on centroid size (Klingenberg 1996) in TpsRegr, ver. 1.36.

The complexity of 2D valve outlines was expressed as 1-circularity. In other words, the more the outline deviated from the shape of a circle, the lower the value of circularity (Osserman 1978). The isoperimetric quotient, evaluating circularity of outlines, is defined as $Q = 4\pi A/P^2$, where A is area enclosed by perimeter P. Thus, Q may be maximally equal to 1.0, attained when the shape is a circle (Osserman 1978). Perimeter (P) was counted as a sum of Euclidean distances between neighbouring landmarks along the out-line in the configurations of 32 landmarks and A was then estimated as an area of a polygon formed by the landmarks. The relationship between circularity and valve size (cen-troid size) was tested using polynomial regression analysis in PAST, ver. 2.17c (Hammer et al. 2001).

To analyse morphological variability (disparity) of the valves, the Procrustes distances of individual objects from the reference forms were computed from landmark con-figurations (Foote 1993). The Procrustes distances were summed for each size group and in each strain separately using TpsSmall, ver. 1.20. The relationship between dis-parity and valve size (centroid size) was tested using poly-nomial regression analysis in PAST, ver. 2.17c (Hammer et al. 2001).

The following analyses were conducted in order to decompose the symmetric and asymmetric compo-nents of the shape variability. We applied the method described by Savriama & Klingenberg (2011) using non-symmetrized landmark configurations. Valve outlines of the studied strains are symmetrical across two orthogonal axes, thus they are designated biradially symmetric. Two

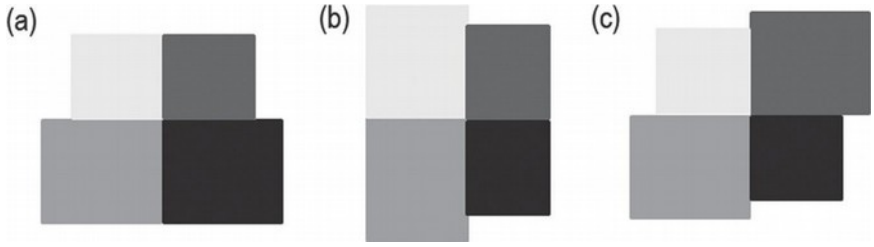

Fig. 1. Symmetry transformations. (a) vertical (heteropolar) type; (b) horizontal (dorsiventral) type; (c) transversal (sigmoid) type. Apical axis of cells corresponds to the y-axis.

perpendicular axes of symmetry were used to partition the configuration into four parts. The studied dataset consisted of the original configurations and the relabelled configurations reflected along the transapical axis, apical axis and the transapical + apical axes (Savriama et al. 2010, Neustupa 2013). As a result, each specimen was characterized by four configurations and their average shape was perfectly symmetrical (Savriama & Klingenberg 2011). The combined dataset consisted of 4 × 149 = 596 *L. dismutica* 1 objects, 4 × 169 = 676 *L. dismutica* 2 objects, 4 × 125 = 500 *N. cryptocephala* objects, and 4 × 125 = 500 *S. pupula* objects. The principal component analysis (PCA) of the original and the rotated/relabelled configurations yields components that clearly separate individual segments of the asymmetric variation (Savriama & Klingenberg 2011). In objects with a biradially symmetric arrangement, the asymmetric vari-ation can be decomposed into three components, namely asymmetry along the apical axis (vertical asymmetry, heteropolar cells), asymmetry along the transapical axis (horizontal asymmetry, dorsiventral cells) and asymmetry along the transversal axis (transversal asymmetry, sigmoid cells), (Fig. 1). In this study, the quantities of asymme-try in individual asymmetric components were assessed by using a separate set of PCAs of the four configurations originating from each object (the original and the three reflected/relabelled configurations). PCAs were based on the variance–covariance matrices of the Procrustes aligned coordinates. Each PCA yielded three axes, illustrating three asymmetrical components. The absolute values of the scores of the original configuration on each of these three components were used as measurements of the asymmetrical variation in each cell. The generalized Procrustes analysis (GPA) and PCA were conducted in package *shapes* ver. 1.0.9 (Dryden & Mardia 1998) in R ver. 2.13.0 (R Development Core Team 2011). Separately, relative proportions of individual asymmetrical components in each cell were assessed as percentages of the explained varia-tion spanned by the individual PC axes. The Friedman test and *post hoc* pairwise comparisons (Wilcoxon's test) were used to evaluate differences among values of asymmetrical components acquired from individual valve landmark configurations of individual strains. The resulting data on the absolute and relative asymmetric variation, in all studied strains, were used to assess differences among the cells.

The relationship between centroid size and asymmetry val-ues was tested using the polynomial regression analysis in PAST, ver. 2.17 (Hammer et al. 2001).

Results

During the vegetative cell division phase of the life cycle, the valve sizes of all four strains changed significantly. The valve size in *Luticola* 1 decreased to 40–50%, in *Luti-cola* 2 to 30–40% (Fig. 2), in *Navicula* to 50–60%, and in *Sellaphora* to 50–60% from the original size (Table 1). The change in valve size was accompanied by a parallel change in the shape of the valves. The multi-variate regression analysis of the shape coordinates on centroid size revealed that size diminution accounted for the notable proportions of the overall shape variations present in all four strains (Table 2). The regression mod-els explained 67% of the total variation in *Luticola* 1, 83% in *Luticola* 2, 66% in *Navicula* and 70% in *Sellaphora*, respectively.

The RW1 scores of the cells from each strain repre-sented the ontogenetic allometric trends throughout the vegetative cell division phase (Figs 3–6). RW 1 axes in all ordinations were strongly dominated with respect to described variation. They accounted for more than 95% of variability in all four strains. RW 1 corresponded to the roundness of the valves in all four strains, while the sec-ond relative warp (RW2) corresponded to the broadness and roundness of the poles relative to the whole valve. Despite these common characteristics, differing shape pat-terns were identified in each strain. The valve outline shape variability, along RW1 in both *Luticola* strains, varied between an elongated shape with a swollen central part and an elliptical shape with a tapered central part (Figs 3– 4). Along RW2, the valve outline varied between valves with rounded apical parts and swollen central part, and valves with a lanceolate shape. In the *Navicula* strain, RW1 corresponded to the width of valves and RW2 cor-responded to the width of the apical parts (Fig. 5). In the *Sellaphora* strain, the valve shape varied between an elon-gated elliptical shape and rounded shape along the RW. RW2 corresponded to the variability between valves with rounded apices and straight central parts, and elliptical valves with narrower apices and rather convex central parts (Fig. 6).

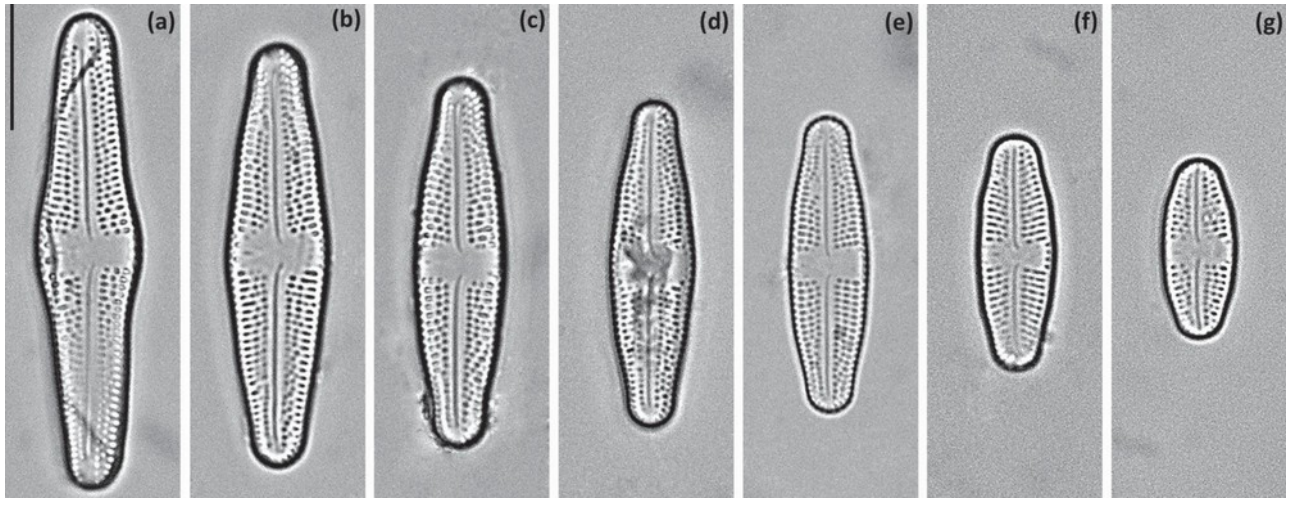

Fig. 2. Representative cells in the size diminution series of *Luticola* 2 strain. Each cell falls into a single-size group (sg). (a) sg 1; (b) sg 2; (c) sg 3; (d) sg 4; (e) sg 5; (f) sg 6; and (g) sg 7. Scale bar = 10 μm.

Table 2. The relative warps analyses and the multivariate regression of shape coordinates on centroid size.

	RWA (% of explained variation by individual RWs)		Shape-size regression		
Strain	RW1	RW2	% explained	Wilks' lambda	*p*-Value
Luticola 1	98.70	0.73	67.00	0.12	< .001
Luticola 2	99.04	0.57	83.00	0.06	< .001
Navicula	96.98	1.54	66.00	0.29	< .001
Sellaphora	99.25	0.40	70.00	0.11	< .001

The analyses of circularity in all four strains favoured a second-order polynomial rather than a linear fit (Table 3). In all four strains, the circularity increased with decreasing size. In *Luticola* 2, *Navicula*, and *Sellaphora*, the minimum circularity values occurred in the biggest valves and the circularity then increased and the maximum values were reached in the smallest valves. However, in *Luticola* 1, circularity had the lowest values in the intermediate stages of the life cycle. Then, this parameter increased (i.e. frustule shape complexity increased) in smaller valves (Fig. 7). The *Sellaphora* strain presented the most gradual increase in circularity in comparison to the other strains.

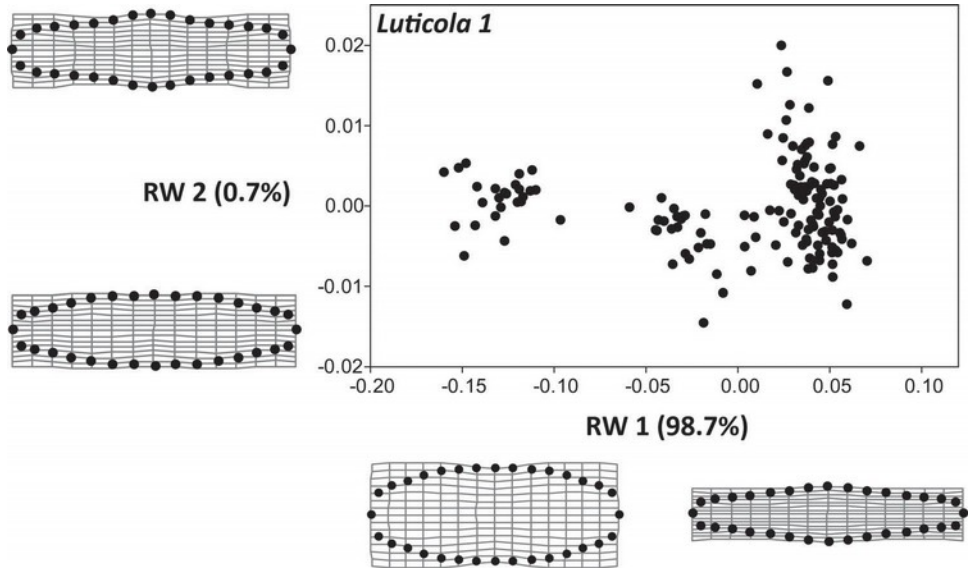

Fig. 3. Ordination plot of the second (RW2) vs. first (RW1) relative warps in the strain *Luticola* 1 representing the shape differences between the valves. Thin-plate splines represent the margins of the realized morphospace on a particular warp.

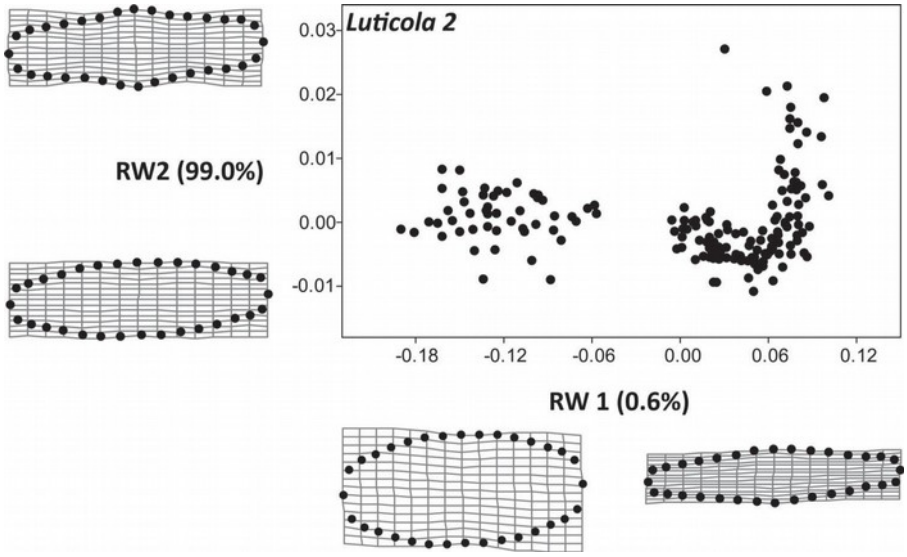

Fig. 4. Ordination plot of the second (RW2) vs. first (RW1) relative warps in the strain *Luticola* 2 representing the shape differences between the valves. Thin-plate splines represent the margins of the realized morphospace on a particular warp.

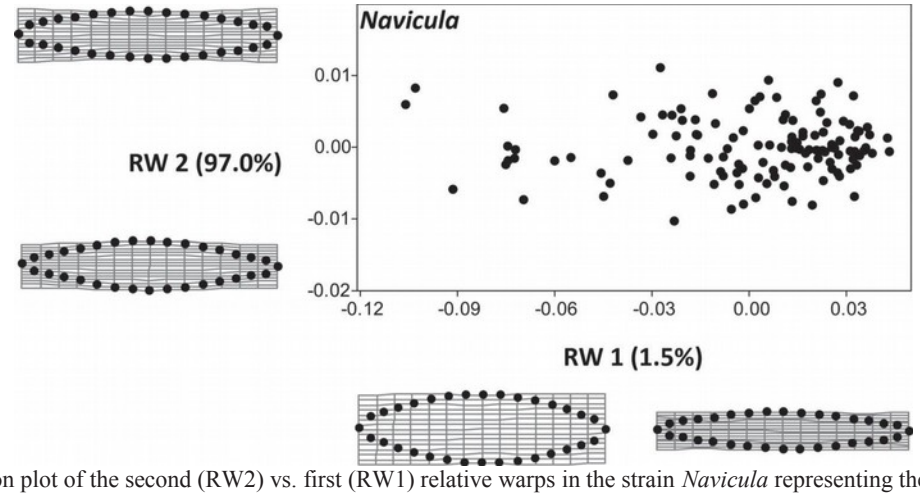

Fig. 5. Ordination plot of the second (RW2) vs. first (RW1) relative warps in the strain *Navicula* representing the shape differences between the valves. Thin-plate splines represent the margins of the realized morphospace on a particular warp.

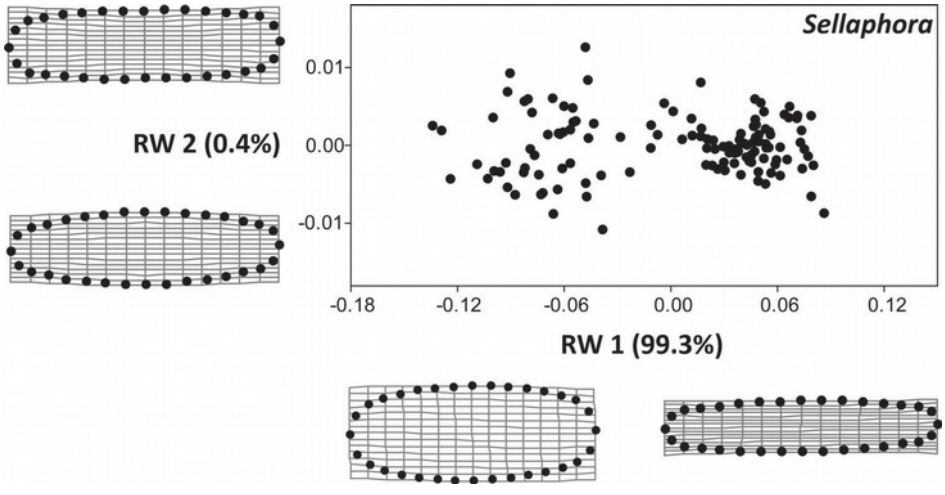

Fig. 6. Ordination plot of the second (RW2) vs. first (RW1) relative warps in the strain *Sellaphora* representing the shape differences between the valves. Thin-plate splines represent the margins of the realized morphospace on a particular warp.

Table 3. The regression analyses of asymmetry, disparity, and circularity versus centroid size.

Strain	Type of analysis	First-order regression			Second-order regression		
		R^2	*p*-Value	*F*	R^2	*p*-Value	*F*
Luticola 1	horizontal asymmetry	0.06	< .01	9.34	0.09	< .001	6.91
	vertical asymmetry	0.02	n.s.	3.68	0.02	n.s.	1.83
	transversal asymmetry	0.07	< .01	10.98	0.07	< .01	5.50
	disparity	0.0005	n.s.	0.08	0.0005	n.s.	0.04
	circularity	0.70	< .001	338.78	0.93	< .001	943.88
Luticola 2	horizontal asymmetry	0.001	n.s.	0.17	0.07	< .01	5.81
	vertical asymmetry	0.06	< .01	11.07	0.07	< .01	6.49
	transversal asymmetry	0.08	< .001	13.58	0.08	< .001	7.18
	disparity	0.16	< .001	32.47	0.25	< .001	27.05
	circularity	0.88	< .001	1160.9	0.97	< .001	2956
Navicula	horizontal asymmetry	0.04	< .05	5.26	0.05	n.s.	2.87
	vertical asymmetry	0.06	< .01	7.10	0.13	< .001	9.24
	transversal asymmetry	0.12	< .001	16.16	0.16	< .001	11.51
	disparity	0.30	< .001	50.89	0.35	< .001	32.73
	circularity	0.67	< .001	248.88	0.8	< .001	204.63
Sellaphora	horizontal asymmetry	0.07	< .01	9.10	0.10	< .01	6.56
	vertical asymmetry	0.13	< .001	18.86	0.13	< .001	9.36
	transversal asymmetry	0.08	< .01	10.19	0.08	< .01	5.19
	disparity	0.12	< .001	16.75	0.13	< .001	8.86
	circularity	0.87	< .001	856.57	0.88	< .001	433.31

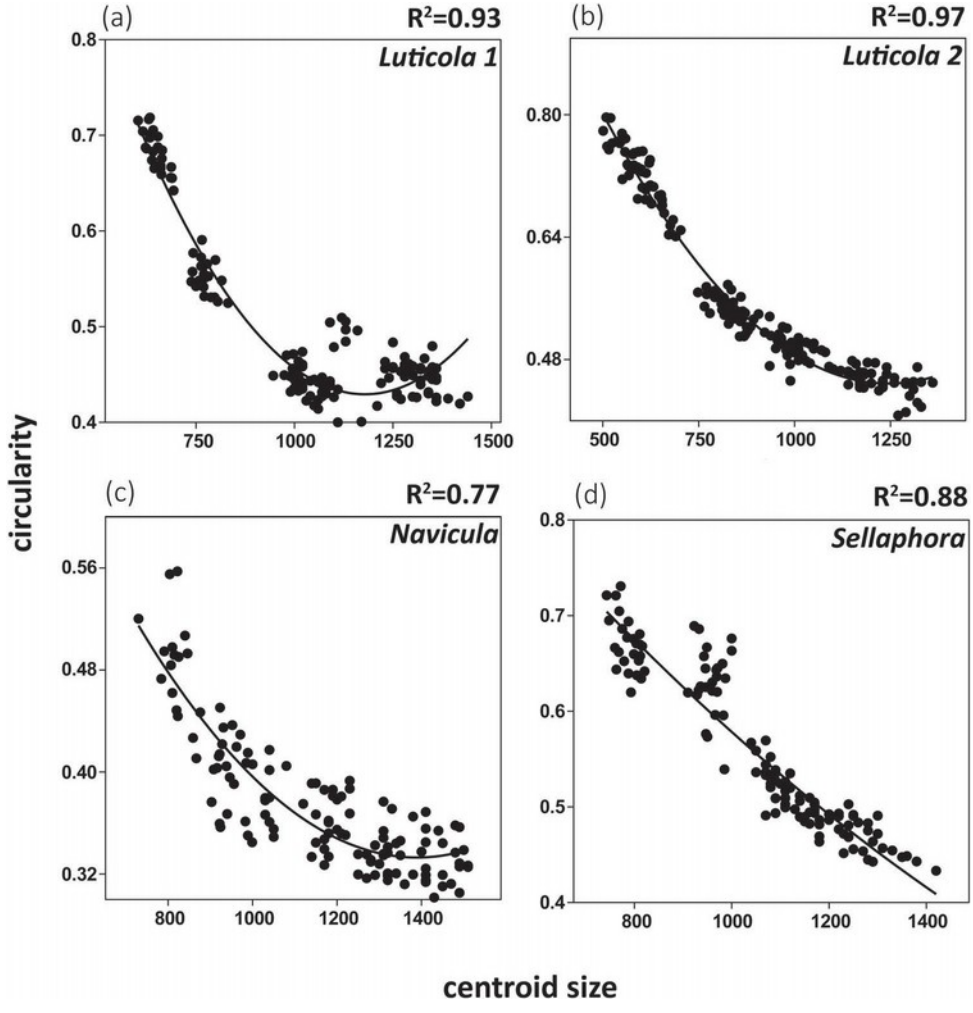

Fig. 7. Jitter plot of second-order regression of circularity versus centroid size. Circularity increases with decreasing size in a nonlinear manner. (a) *Luticola* 1; (b) *Luticola* 2; (c) *Navicula*; and (d) *Sellaphora*.

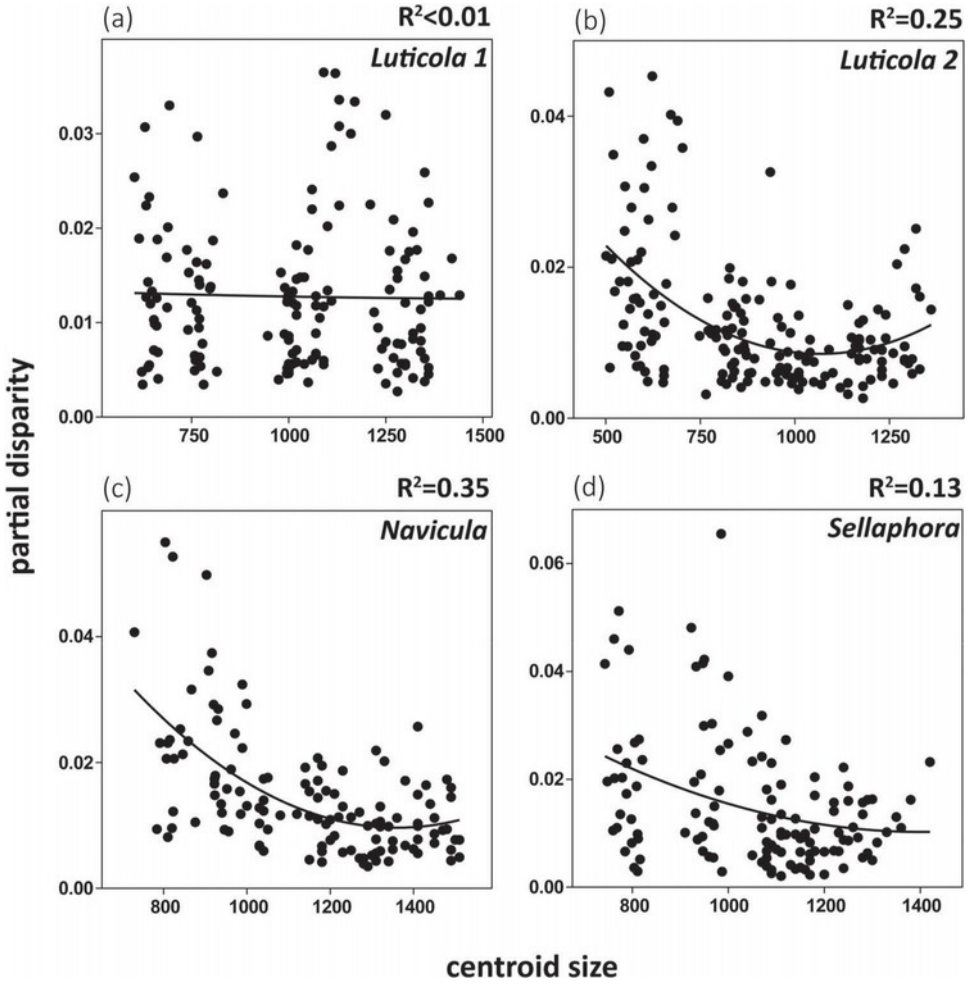

Fig. 8. Jitter plot of second-order regression of tangent Procrustes distances of individual cells to centroids of their respective size groups versus centroid size. Shape variability (disparity) increases with decreasing size. (a) *Luticola* 1; (b) *Luticola* 2; (c) *Navicula*; and (d) *Sellaphora*.

The disparity analysis also favoured the second-order polynomial fit in all strains except *Luticola* 1, in which neither the linear nor the second-order polynomial regression models were significant. In the remaining three strains, the results of the second-order polynomial regression were significant (Table 3). In these three strains, the dispar-ity increase reached its maximum in the smallest valves (Fig. 8).

The asymmetry of landmark configurations did not change explicitly in relation to valve size. The differ-ences among the size groups typically described only small proportions of variation in the observed values of valve asymmetry. Nevertheless, several regression analy-ses of each component of asymmetric variability showed a non-random linear (vertical asymmetry in *Sellaphora*) or quadratic (vertical and transversal asymmetries in *Navic-ula* and horizontal asymmetry in *Luticola* 1 and 2) relation-ship with centroid size (Table 3). However, the coefficients of determination (R^2) were low, especially in comparison with analyses of the relationship of partial disparity or

circularity and the size group rank, and the trends were not uniform, that is, some components of asymmetry increased and some decreased in relation to centroid size in the same strain. The Friedman tests of differences between the individual types of asymmetry within the strains were significant in *Luticola* 2 ($p < .05$) and *Sellaphora* ($p < .001$) strains. In both, the horizontal (dorsiventral) asymmetry component was significantly lower than both remaining components (Fig. 9). In the other two strains, the asymmetric patterns corresponding to heteropolar, dorsiventral, and sigmoid transformations of the ideally symmetric body plan were approximately equal.

Discussion

A quantitative shape analysis revealed similar ontogenetic allometric trends among the different strains and genera. In all four strains, valve outline complexity decreased as the number of vegetative cell divisions increased and was at its lowest at the end of the vegetative cell division

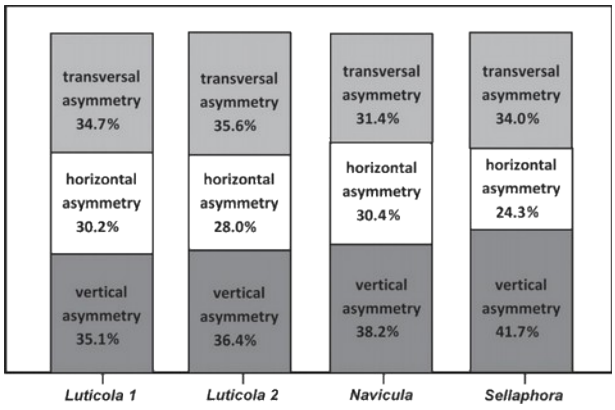

Fig. 9. The proportions of individual types of asymmetry within the strains. Vertical asymmetry – heteropolar type; horizontal asymmetry – dorsiventral type; and transversal asymmetry – sigmoid type.

phase. In other words, the smaller the cells of the stud-ied strains were, the more circular their outlines were. Although there were similarities between the strains, there were also differences in their life cycles and shape dynam-ics. In particular, both *Luticola* strains exhibited patterns different from the other strains. According to our obser-vations, cell size restoration in *Navicula* and *Sellaphora* strains occurred when the cells reached 50–60% of their original size. However, both *Luticola* 1 and *Luticola* 2 ini-tiated sexual reproduction when they reached 40–50% and 30–40% of their original sizes, respectively (Poulícková ˇ & Mann 2006, Poulícková ˇ 2008). The initial cells of *Luticola* resemble the shape of their auxospores with a typical cen-tral swelling (Poulícková ˇ 2008). These centrally swollen initial cells become narrower after a few divisions, as reported by Geitler (1932). The specific rounded shape of the initial cells may explain the high circularity that occurs in the biggest size group (Fig. 7). On the other hand, the ini-tial and post-initial cells of the *Navicula* cells do not exhibit any swelling, despite their centrally swollen auxospore (Poulícková ˇ & Mann 2006). Consequently, the circularity was the lowest in the biggest size group (Fig. 7). *Sell-aphora* cells do not have any swelling of the auxospores or the initial cells (Mann 1989), and the circularity values in all five size groups were consistent with this.

It has been proposed that size can influence the physical conditions of a cell's internal environment and the organi-zation of its organelles (Geitler 1932, Schmid 1994). As the space inside the frustule decreases, the viscosity, surface tension, and pressure increase (Geitler 1932). The surface-to-volume (S-to-V) ratio of isometrically scaled objects increases with decreasing size. In other words, the cell volume decreases more rapidly than the surface (Thomp-son 1917). However, the cell size diminution in pennate diatoms is accompanied by allometric shape changes of the cells (Geitler 1932). According to our results, cell shape simplifies with an increasing number of cell divisions, so the change in the S-to-V ratio is probably not that profound. The S-to-V ratio may be influenced by the pos-sible changes in cingulum height throughout the vegetative cell division phase. Geitler (1932) mentioned that there is no strong correlation between cell length and cingu-lum height. According to his observation, cingulum height may even increase slightly as cell length decreases (Geitler 1932). Geitler's hypotheses are supported by a morpho-metric study of *Diatoma moniliformis* (Kützing) D. M. Williams populations in natural conditions (Potapova & Snoeijs 1997). According to the above-mentioned authors, a decrease in the apical axis is inevitable; however, the transapical and pervalvar axes can be modified, especially because the diatom girdle is much more flexible than the thecae. Thus, we conclude that potential changes in cingu-lum height may contribute to a deceleration of the S-to-V ratio of the studied strains throughout the vegetative cell division phase.

Even though cell complexity of the populations decreased during the size diminution phase, disparity (shape variability) increased. Given the genetic homogene-ity of our strains, this pattern could not be ascribed to any hypothetical shifts between different genotypes pro-ducing different morphologies during the vegetative cell division phase. Conversely, the observed disparity patterns within the clonal populations should be treated as specific examples of structural inheritance (Jablonka & Raz 2009). According to the qualitative observations based on light and electron microscopy, diatom parental cells serve as a mould for the circumferential outline of newly formed hypothecae during vegetative cell division. Consequently, some slight morphological deviations can be passed on to other generations (Crawford 1981, Schmid 1986, Schmid 1994). This could explain the pattern of increasing phe-notypic plasticity in our strains, namely the accumulating inaccuracies resulting in shape variety within a popula-tion. We propose that the observed, consistent increase in morphological disparity of the studied populations might illustrate a more general pattern exhibited by diatom pop-ulations that results from their unique mechanism of cell wall morphogenesis and vegetative inheritance.

Our test of asymmetry components and their contri-bution to the overall asymmetry revealed that, in two out of four strains (*Luticola* 2 and *Sellaphora*), the horizon-tal (dorsiventral) asymmetry was significantly lower than the other components. In the remaining strains, the dif-ferences between the asymmetry components were not significant, that is, the asymmetric components in these strains were balanced. This is strikingly different from the pattern in desmids (Savriama et al. 2010, Neustupa 2013), another microalgal group with complex cellular symme-try. These charophyte algae possess cell halves (semi-cells) that form at different times and therefore can form under different environmental conditions. Thus, their asymmetric variation is dominated by upper–lower shape differences, which highlights the contrast between the semi-cells. The

silica deposition process in diatoms is not simultaneous but sequential (Mann 1981). The raphe system is deposited first on one side of the valve (the primary side) and then on the other (the secondary side).When the last part of the raphe is defined, two discontinuities remain (Voigt dis-continuities), (Mann 1981). Despite these irregularities, we did not detect any signal in our data that would indicate increased left–right asymmetry (i.e. differences between the primary and secondary sides of the valve).

During the vegetative cell division phase of the life cycle, the level of asymmetry remained rather constant. In contrast to increasing disparity, asymmetry did not change consistently in relation to size. The slight asymmetry of the valves can therefore be considered an intrinsic prop-erty of diatom cell morphology, regardless of the number of preceding vegetative cell divisions. The decomposition of individual segments of asymmetry was conducted fol-lowing a modified protocol based on Savriama et al. (2010) and Savriama & Klingenberg (2011). As in these studies, as well as in Neustupa (2013) and Savriama et al. (2015), it was based on the general Procrustes superimposition of the symmetry group formed by the transformations of the original configurations of the landmarks spanning the outline of the valves. Thus, in a biradially symmetric 2D object, such as the pennate diatom valve, there were four symmetry transformations forming the symmetry group (Klingenberg 2015).

However, our asymmetry analysis differed from those mentioned above because it always considered one con-figuration at a time. Thus, the Procrustes superimposition was conducted separately for each set of the original and the transformed configurations of the landmarks describ-ing the shape properties of a single valve. This approach is very similar to general protocols described by Zabrodsky et al. (1992, 1995) and Graham et al. (2010) for the anal-ysis of the amounts of continuous symmetry in configura-tions defined by a set of homologous points. Klingenberg (2015) pointed out that this approach, while mathemati-cally correct, has no way of distinguishing fluctuating and directional asymmetry. However, in unicellular organisms with biradially symmetrical cells, the repeated parts are usually unsigned, that is, their left and right, or top and bottom cellular halves cannot be distinguished (Fránková et al. 2009, Savriama et al. 2010, Neustupa 2013). This is also the case for many diatoms and, therefore, our analysis was based on the decomposition of the total cellular asym-metry into three segments that correspond to the bending of the horizontal and vertical axes of valve symmetry. However, it did not use the concepts of fluctuating and directional asymmetry. Zabrodsky et al. (1992, 1995) used their methodology in chemistry, for the identification of the different types of symmetry optimally fitting a set of points, such as positions of individual atoms in a molecule. In fact, this is also applicable to diatom valves, as a way of looking for the best fitting form of valve asymmetry. Given different evolutionary or ecological hypotheses, an analysis of the proportions of the asymmetric variation corresponding to the heteropolar, dorsiventral, and sigmoid patterns in individual cells may be of interest.

Additionally, another difference between the one-by-one asymmetry decomposition used in this study and the joint Procrustes analysis of large sets of the original and the transformed configurations is the elimination of the entirely symmetric variation that typically describes the among-individual variances (Savriama et al. 2010, Neustupa 2013). The joint Procrustes approach typically assigns large proportions of the total variation to a variation that is identical in all repeated parts, but differs among the individuals. This segment of variation inherently increases in relation to the size of the dataset and, thus, in rela-tion to its total morphological variability. Therefore, the joint Procrustes approach would not allow for the quan-titative comparison of the asymmetric variations among datasets with different numbers of individuals, such as those acquired in different studies or experimental designs.

As shown elsewhere (Potapova & Hamilton 2007, Veselá et al. 2009, English & Potapova 2012, Edgar et al. 2015), geometric morphometrics has a great potential for application in various areas of diatomology (for detailed review see Pappas et al. 2014). It enables a researcher to quantify and analyse slight morphological differences that cannot be captured by microscopic observation. The geometric morphometric techniques can reveal distinct dif-ferences between morphs in diatom samples that were traditionally assigned to single species (Van de Vijver et al. 2013). Traditional measurements may be biased by the omnipresent size diminution, which can outweigh the shape differences. On the other hand, geometric morpho-metrics studies size-free variation, and thus it is possible to discriminate between two species at different stages of their vegetative life cycle (Veselá et al. 2009). The shape changes related to size can even serve as a sig-nal when exploring diatom species diversity because dif-ferent species can have dissimilar allometric trajectories (English & Potapova 2012). As illustrated in this study, shape variability and dynamics in clonal populations can be used to explore phenotypic plasticity and its evolution-ary implications. The morphological variation and asym-metry of diatom valves at the population level can be studied in relation to environmental conditions or stress factors (Potapova & Hamilton 2007). Thus, diatoms, with their rigid silica frustules, are ideal model organisms for quantitative morphometric studies focused on free-living cells.

Acknowledgements

The author is grateful to Prof. Aloisie Poulícková˘ for provid-ing four strains of raphid diatoms used in this study. The author also thanks the anonymous reviewers of Diatom Research and the editor, Dr. Eileen J. Cox, for their critical comments on the manuscript that had led to significant improvements of the final text.

Funding

The study was funded by the Faculty of Science of the Charles University in Prague. The English language and style corrections were made by Editage.

References

ADAMS D.C., ROHLF F.J. & SLICE D.E. 2004. Geometric morphometrics: ten years of progress following the 'revolution'. *Italian Journal of Zoology* 71: 5–16.

ANDERSEN R.A. (Ed.). 2005. *Algal culturing techniques*. Elsevier Academic Press, London. 578 pp.

BOOKSTEIN F.L. 1997. *Morphometric tools for landmark data: geometry and biology*. Cambridge University Press, Cambridge. 436 pp.

COX E.J. 1986. Some taxonomic and ecological considerations of morphological variation within natural populations of benthic diatoms lles. In *Proceedings of the 8th Diatom-Symposium, Paris 1984* (Ed. by M. RICARD), pp. 163–172. O. Koeltz, Koenigstein.

COX E.J. 1993. Diatom systematics – a review of past and present practice and a personal vision for future development. *Beihefte zur Nova Hedwigia* 106: 1–20.

CRAWFORD R.M. 1981. Some considerations of size reduction in diatom cell walls. In *Proceedings of the 6th international diatom symposium* (Ed. by R. ROSS), pp. 253–265. O. Koeltz, Koenig-stein.

DREBES G. 1977. Sexuality. In *The biology of diatoms* (Ed. by D. WERNER), pp. 250–283. University of California Press, Berkeley, California.

DRYDEN I.L. & MARDIA K.V. 1998. *Statistical analysis of shape*. John Wiley & Sons, New York. 347 pp.

EDGAR R.K., SALEH A.I. & EDGAR S.M. 2015. A morphometric diagnosis using continuous characters of *Pinnunavis edkuensis, sp. nov.* (Bacillariophyta: Bacillariophyceae), a brackish-marine species from Egypt. *Phytotaxa* 212: 1–56.

EDLUND M.B. & STOERMER E.F. 1997. Ecological, evolutionary, and systematic significance of diatom life history. *Journal of Phycology* 33: 897–918.

ENGLISH J.D. & POTAPOVA M.G. 2012. Ontogenetic and interspecific valve shape variation in the Pinnatae group of the genus *Surirella* and the description of *S. lacrimula* sp. nov. *Diatom Research* 27: 9–27.

FOOTE M. 1993. Contributions of individual taxa to overall morphological disparity. *Paleobiology* 19: 403–419.

F RÁNKOVÁ M., P OULÍCKOVÁ A., N EUSTUPA J., P ICHRTOVÁ M. & MARVAN P. 2009. Geometric morphometrics – a sensitive method to distinguish diatom morphospecies: a case study on the sympatric populations of *Reimeria sinuata* and *Gomphonema tergestinum* (Bacillariophyceae) from the River Becva,˘ Czech Republic. *Nova Hedwigia* 88: 81–95.

GEITLER L. 1932. Der Formwechsel der pennaten Diatomeen (Kieselalgen). *Archiv fur Protistenkunde* 78: 1–226.

GRAHAM J.H., RAZ S., HEL-OR, H. & NEVO E. 2010. Fluctuating asymmetry: methods, theory, and applications. *Symmetry* 2: 466–540.

HAMMER O., HARPER D.A.T. & RYAN P.D. 2001. PAST: Paleontological statistics software package for education and data analysis. *Palaeontologia Electronica* 4: 9. http://palaeo-electronica.org/2001_1/past/issue1_01.htm.

JABLONKA E. & RAZ G. 2009. Transgenerational epigenetic inheritance: prevalence, mechanisms, and implications for the study of heredity and evolution. *The Quarterly Review of Biology* 84: 131–176.

KLINGENBERG C.P. 1996. Multivariate allometry. In *Advances in morphometrics* (Ed. by L.F. MARCUS), pp. 23–49. Plenum Press, New York.

KLINGENBERG C.P. 2015. Analyzing fluctuating asymmetry with geometric morphometrics: concepts, methods, and applications. *Symmetry* 7: 843–934.

KLINGENBERG C.P., BARLUENGA M. & MEYER A. 2002. Shape analysis of symmetric structures: quantifying variation among individuals and asymmetry. *Evolution* 56: 1909–1920.

KOCIOLEK J.P. & STOERMER E.F. 2010. Variation and polymorphism in diatoms: the triple helix of development, genet-ics and environment. A review of the literature. *Vie et Milieu* 60: 75–87.

LEWIS W.M. JR. 1984. The diatom sex clock and its evolutionary significance. *The American Naturalist* 123: 73–80.

MACDONALD J.D. 1869. On the structure of diatomaceous frustule, and its genetic cycle. *Annals and Magazine of Natural History* 3: 1–8.

MANN D.G. 1981. A note on valve formation and homology in the diatom genus *Cymbella*. *Annals of Botany* 47: 267–269.

MANN D.G. 1989. The diatom genus Sellaphora: separation from *Navicula*. *British Phycological Journal* 24: 1–20.

MANN D.G. 1999. The species concept in diatoms. *Phycologia* 38: 437–495.

MANN D.G. & CHEPURNOV V.A. 2005. Auxosporulation, mating system, and reproductive isolation in *Neidium* (Bacillar-iophyta). *Phycologia* 44: 335–350.

MANN D.G., MCDONALD S.M., BAYER M.M., DROOP S.J.M., CHEPURNOV V.A., LOKE R.E., CIOBANU A. & DU BUF J.M.H. 2004. The *Sellaphora pupula* species complex (Bacillariophyceae): morphometric analysis, ultra-structure and mating data provide evidence for five new species. *Phycologia* 43: 459–482.

MOU D. & STOERMER E.F. 1992. Separating *Tabellaria* (Bacillariophyceae) shape groups based on Fourier descriptors. *Journal of Phycology* 28: 386–395.

NEUSTUPA J. 2013. Patterns of symmetric and asymmetric morphological variation in unicellular green microalgae of the genus *Micrasterias* (Desmidiales, Viridiplantae). *Fottea* 13: 53–63.

OSSERMAN R. 1978. The isoperimetric inequality. *Bulletin of the American Mathematical Society* 84: 1182–1238.

PAPPAS J.L. & STOERMER E.F. 2003. Legendre shape descriptors and shape group determination of specimens in the *Cymbella cistula* species complex. *Phycologia* 42: 90–97.

PAPPAS J.L., FOWLER G.W. & STOERMER E.F. 2001. Calculating shape descriptors from Fourier analysis: shape analysis of *Asterionella* (Heterokontophyta, Bacillariophyceae). *Phycologia* 40: 440–456.

PAPPAS J.L., KOCIOLEK J.P. & STOERMER E.F. 2014. Quantitative morphometric methods in diatom research. *Nova Hedwigia, Beiheft* 143: 281–306.

PFITZER E. 1869. Über den Bau und die Zellteilung der Diatomeen. *Botanische Zeitung* 27: 774–776.

POTAPOVA M. & SNOEIJS P. 1997. The natural life cycle in wild populations of *Diatoma moniliformis* (Bacillariophyceae)

and its disruption in an aberrant environment. *Journal of Phycology* 33: 924–937.

POTAPOVA M. & HAMILTON P.B. 2007. Morphological and ecological variation within the *Achnanthidium minutissimum* (Bacillariophyceae) species complex. *Journal of Phycology* 43: 561–575.

OULÍCKOVÁ A. 2008. Morphology, cytology and sexual reproduction in the aerophytic cave diatom *Luticola dismutica* (Bacillariophyceae). *Preslia* 80: 87–99.

OULÍCKOVÁ A. & MANN D.G. 2006. Sexual reproduction in *Navicula cryptocephala* (Bacillariophyceae). *Journal of Phycology* 42: 872–886.

R DEVELOPMENT CORE TEAM. 2011. *R: A language and environment for statistical computing*. R Foundation for Statistical Computing, Vienna. https://www.r-project.org/foundation/.

RHODE K.M., PAPPAS J.L. & STOERMER E.F. 2001. Quantitative analysis of shape variation in type and modern populations of *Meridion* (Bacillariophyceae). *Journal of Phycology* 37: 175–183.

ROHLF F.J. 2013. *TPS software series*. Department of Ecology and Evolution, State University of New York, Stony Brook.

ROSE D.T. & COX E.J. 2014. What constitutes *Gomphonema parvulum?* Long-term culture studies show that some varieties of *G. parvulum* belong to other *Gomphonema* species. *Plant Ecology and Evolution* 147: 366–373.

ROUND F.E., CRAWFORD R.M. & MANN D.G. 1990. *The diatoms: biology and morphology of the Genera*. Cambridge University Press, Cambridge. 131 pp.

SAVRIAMA Y. & KLINGENBERG C.P. 2011. Beyond bilateral symmetry: geometric morphometric methods for any type of symmetry. *BMC Evolutionary Biology* 11: 280.

SAVRIAMA Y., NEUSTUPA J. & KLINGENBERG C.P. 2010. Geometric morphometrics of symmetry and allometry in *Micrasterias rotata* (Zygnemophyceae, Viridiplantae). *Nova Hedwigia* 136: 43–54.

SAVRIAMA Y., STIGE L.C., GERBER S., PÉREZ T., ALIBERT P. & DAVID B. 2015. Impact of sewage pollution on two species of sea urchins in the Mediterranean Sea (Cortiou, France): Radial asymmetry as a bioindicator of stress. *Ecological Indicators* 54: 39–47.

SCHMID A.M. 1986. Organization and function of cell structures in diatoms and their morphogenesis. In: *Proceedings of the 8th International Diatom Symposium* (Ed. by M. RICARD), pp. 271–292. O. Koeltz, Koenigstein.

SCHMID A.M. 1994. Aspects of morphogenesis and function of diatom cell walls with implications for taxonomy. *Protoplasma* 181: 43–60.

THERIOT E. & LADEWSKI T.B. 1986. Morphometric analysis of shape of specimens from the neotype of *Tabellaria flocculosa* (Bacillariophyceae). *American Journal of Botany* 73: 224–229.

THERIOT E., HÅKANSSON H. & STOERMER E.F. 1988. Morphometric analysis of *Stephanodiscus alpinus* (Bacillariophyceae) and its morphology as an indicator of lake trophic status. *Phycologia* 27: 485–493.

THOMPSON D'ARCY W. 1917. *On growth and form*. Cambridge University Press, Cambridge. 793 pp.

TROPPER C.B. 1975. Morphological variation of *Achnanthes hauckiana* (Bacillariophyceae) in the field. *Journal of Phy-cology* 11: 297–302.

VAN DE VIJVER B., MORAVCOVA A., KUSBER W.H. & NEUSTUPA J. 2013. Analysis of the type material of *Pin-nularia divergentissima* (Grunow in Van Heurck) Cleve (Bacillariophyceae). *Fottea* 13: 1–14.

VESELÁ J., NEUSTUPA J., PICHRTOVÁ M. & OULÍCKOVÁ A. 2009. Morphometric study of *Navicula* morphospecies (Bacillariophyta) with respect to diatom life cycle. *Fottea* 9: 307–316.

ZABRODSKY H., PELEG S. & AVNIR D. 1992. Continuous symmetry measures. *Journal of the American Chemical Society* 114: 7843–7851.

ZABRODSKY H., PELEG S. & AVNIR D. 1995. Symmetry as a continuous feature. *IEEE Transactions on Pattern Analysis and Machine Intelligence* 17: 1154–1166.

ZELDITCH M.L., SWIDERSKI D.L., SHEETS H.D. & FINK W.L. 2004. *Geometric morphometrics for biologists*. Elsevier Academic Press, New York. 443 pp.